

Studying fission neutrons with 2E-2v and 2E

Ali Al-Adili^{1,*}, Kaj Jansson¹, Diego Tarrío¹, Franz-Josef Hamsch², Alf Göök², Stephan Oberstedt², Marc Olivier Frégeau³, Cecilia Gustavsson¹, Mattias Lantz¹, Andrea Mattera¹, Alexander V. Prokofiev¹, Vasileios Rakopoulos¹, Andreas Solders¹, Marzio Vidali², Michael Österlund¹, and Stephan Pomp¹

¹Department of Physics and Astronomy, Uppsala University, Sweden

²European Commission, Joint Research Centre, Directorate G-2, Geel, Belgium

³GANIL CEA/DRF-CNRS/IN2P3, Caen, France

Abstract. This work aims at measuring prompt-fission neutrons at different excitation energies of the nucleus. Two independent techniques, the 2E-2v and the 2E techniques, are used to map the characteristics of the mass-dependent prompt fission neutron multiplicity, $\bar{\nu}(A)$, when the excitation energy is increased.

The VERDI 2E-2v spectrometer is being developed at JRC-GEEL. The Fission Fragment (FF) energies are measured using two arrays of 16 silicon (Si) detectors each. The FFs velocities are obtained by time-of-flight, measured between micro-channel plates (MCP) and Si detectors. With MCPs placed on both sides of the fission source, VERDI allows for independent timing measurements for both fragments. $^{252}\text{Cf}(\text{sf})$ was measured and the present results revealed particular features of the 2E-2v technique. Dedicated simulations were also performed using the GEF code to study important aspects of the 2E-2v technique. Our simulations show that prompt neutron emission has a non-negligible impact on the deduced fragment data and affects also the shape of $\bar{\nu}(A)$. Geometrical constraints lead to a total-kinetic energy-dependent detection efficiency.

The 2E technique utilizes an ionization chamber together with two liquid scintillator detectors. Two measurements have been performed, one of $^{252}\text{Cf}(\text{sf})$ and another one of thermal-neutron induced fission in $^{235}\text{U}(\text{n},\text{f})$. Results from $^{252}\text{Cf}(\text{sf})$ are reported here.

1 Introduction

The evolution of the fragment-specific neutron-multiplicity, $\bar{\nu}(A)$, as a function of excitation energy, is an important observable. It reflects the sharing of the total excitation energy (TXE) and how nuclear shell effects wash out at higher excitation energy. Some works (theoretical as well as experimental) assume a higher $\bar{\nu}(A)$ for all fragments as excitation energy increases. However, the few available experimental data sets contradict this and instead point to an increase of $\bar{\nu}(A)$ only for heavy fragments [1]. Hence, more attention needs to be drawn to resolve this question and arrive at a proper description for the excitation energy dependence of $\bar{\nu}(A)$.

In this paper two different methods are being used with the aim to study this matter, in the first chance fission of $^{235}\text{U}(\text{n},\text{f})$. To realize this goal, $^{252}\text{Cf}(\text{sf})$ is used for development and calibration

*e-mail: ali.al-adili@physics.uu.se

purposes. In the so-called "2E-2v" method, we measure both fragments' velocities and energies, simultaneously. By using these four observables, one can attempt to derive the fission fragment pre- and post-neutron emission masses. The average neutron multiplicity, $\bar{\nu}(A)$, is thus obtained as the difference of the pre- and post-neutron emission masses on an event-by-event basis. In the "2E" method, both fragments' kinetic energies are measured simultaneously. To determine $\bar{\nu}(A)$, neutron detectors (ND) are added to measure the rate of coincidences, between the fission chamber and the NDs. The experimental setups of both systems are sketched in Fig. 1.

2 Double-energy double-velocity method (2E-2v)

Currently, a few 2E-2v-instruments are being developed across the world, e.g., FALSTAFF, SPIDER, STEFF and VERDI [2–5]. One important goal is to suppress uncertainties in fission yield experiments, by enhancing the mass resolution. In principle, the method itself should be able to deliver a mass resolution of 1–2 mass units. The resolution is mainly limited by the neutron boil-off, but additional instrument-dependent effects apply (e.g. energy-losses in targets and foils and energy spreads in Si detectors and ionization chambers). The 2E-2v method has one obvious advantage, namely, that it does not need external input data regarding $\bar{\nu}(A)$, Total Kinetic Energy (TKE) or incident neutron energy (E_n), during analysis. Such data are indispensable input to the 2E method.

2.1 VERDI

The VERDI (VELOCITY foR Direct particle Identification) spectrometer is developed at the JRC-GEEL. The instrument has two independent time-of-flight (TOF) sections, each hosting 16 NTD-Silicon (Si) detectors (PIPS). The velocity of each fragment, respectively its time-of-flight, is measured between either of two MCP and one of the Si detectors. The Si detectors also measure the kinetic energy of the fission fragments. The setup is schematically shown in Fig. 1a.

In a fission event, the released energy (Q) is divided between the TKE and the TXE. The TKE is shared between the nascent fragments according to momentum conservation. The fragments TOF thus decompose into two, overlapping, distributions. The FFs, after neutron emission, exit the target back-to-back and travel towards the Si-detectors. Some electrons are sputtered from the target and get deflected 90° by an electrostatic mirror towards respective MCP. A few electrons are enough to give rise to a start signal for the fragment TOF. The FFs traverse a distance of about 50 cm before reaching the Si detectors with a present size of 450 mm^2 . The Si detectors are of double use: providing both the TOF stop signals and the FFs kinetic energies.

First results from VERDI, using spontaneous fission of ^{252}Cf , were published by Fréreau et al. [5]. Decent results were reported already using one MCP providing a common start signal. Another MCP was installed recently in order to enhance the TOF precision, and to improve the calibration procedure. After installation, a refined data analysis revealed limitations of two of the corrections needed, namely, the energy-calibration, responsible for the pulse-height-defect (PHD) and the plasma delay time (PDT) correction.

The energy-calibration was previously performed using the Schmitt calibration procedure [6]. However, the mean energy values turned out to be too high for ^{252}Cf . Two different methods were tested to remedy this. One was a newly developed iterative Schmidt procedure [7]. The other was simply an adaptation of the adjusted Schmidt values from Müller et al. [8].

The pre-neutron emission mass distributions, integral and as a function of TKE, of the updated VERDI instrument were promising. The mass yield showed an enhanced peak-to-valley ratio and a somewhat narrower distribution (see Fig. 2 for one selected Si detector pair), compared to reference

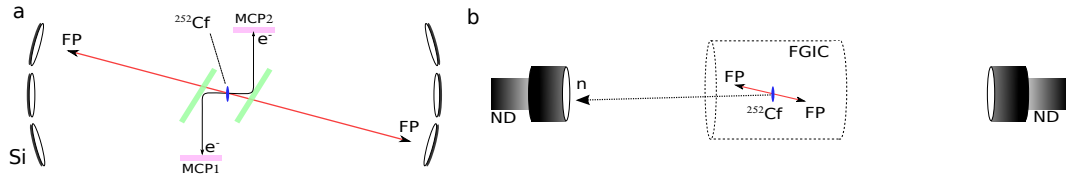


Figure 1. a) Schematics of the VERDI 2E-2v setup, with two arrays of 16 Si detectors and two Micro Channel Plate (MCP) assemblies as signal trigger. b) Schematics of the 2E setup with a Frisch-Grid Ionization Chamber (FGIC) and two liquid scintillator neutron detectors (ND).

2E data [9]. Calculation of the 2v mass yields will cancel some systematic errors, which is why these yields are rather robust against potential problems [10].

The mass-dependent neutron multiplicity shape differed from the 2E data [9], especially around mass symmetry. The more pronounced peaks were first interpreted as a sign of a better mass resolution compared to 2E. A set-back was however encountered in the $\bar{\nu}(TKE)$ shape, which showed the opposite trend of what is expected. Since $Q = TKE - TXE$, the $\bar{\nu}(TKE)$ should have a negative slope, as fewer neutrons are emitted for higher TKE values, i.e., lower TXE values. Our data exhibited a higher $\bar{\nu}$ as a function of TKE which was obviously wrong. The PDT was the prime suspect, as it is a delicate part of the analysis and which relies directly on the related 2E analysis from the silicon detectors.

The measured TOFs are delayed, due to the creation of a plasma in the PIPS detectors. In literature there are contradicting correction methods for this effect [10–12]. The simplified linear relationship ("scaling law") used by Velkovska et al. [11] was initially adopted for VERDI. The measured velocities were plotted as a function of the calculated velocities from the 2E energies. A conventional 2E analysis was performed on the Si energy data providing the "true" velocities. The velocity plot was linearly fitted to provide the "true" velocity as a function of the measured one. However, this method seems to contradict the PDT-systematics of Bohne et al. [12]. And indeed, the application of the scaling law produced unphysical results based on the VERDI data.

A preliminary analysis was recently done, using a new PDT-correction method. The PDT was parameterized as a function of pre-neutron mass and energy. Through an iterative procedure the parameters were improved. As a result from the new approach $\bar{\nu}(TKE)$ showed a more reasonable trend. The obtained VERDI slope corresponds to 13 MeV/n, which agrees rather well with literature data of 12.6 MeV/n [9]. We plan to refine this method by parameterizing the PDT consistently with the systematics of Ref. [12].

2.2 GEF simulations for VERDI

In general, the 2E-2v data suffers from a limited solid angle coverage (1%). This does not only affect statistics, but could also introduce biases caused by the instrument geometry. We know that in about half of the acquired fission events, only one fragment is detected. The other fragment missed the complementary Si detector. To check the effect on fission observables, dedicated simulations were performed. The simulations are based on the GEF event-by-event output. From GEF we obtain information on A and Z for each fragment, their kinetic energies, and information on the emitted secondary particles. We sample the neutron emission isotropically in the center of momentum (CM) frame. The full relativistic kinematics of the fragments and emitted neutrons have been taken into

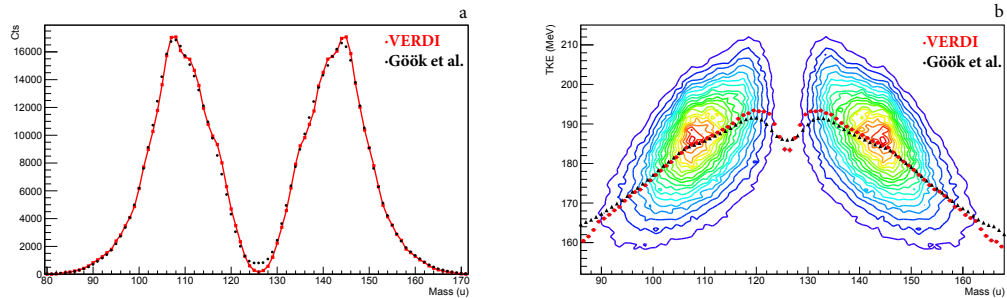


Figure 2. The ^{252}Cf mass (a) and mass vs. TKE (b) in red, for one Si pair, compared to Ref. [9] in black.

account. The relativistic calculations are necessary to prevent systematic errors in the order of 0.1 u compared to classical kinematics.

The simulations help to understand several features of the 2E-2v method. Firstly, the detection efficiency of coincidence events was about half, confirming the VERDI observation. Moreover, the detection efficiency is TKE-dependent as seen in Fig. 3a. For low TKE values, the efficiency becomes as low as 40% while for the highest TKE values it reaches 100%. This is due to neutron emission which increases for lower TKE, giving rise to larger fragment angular deviation from the fission axis. Secondly, a central assumption in 2E-2v is the one on average unchanged fragment velocity, after neutron emission. But since the fragment velocity is conserved only on average, and not for specific events, this could partially wash out fine structures in the mass distribution. This was observed in a pseudo-analysis of the input GEF data. Another consequence of the neutron emission are changes in the sawtooth shape as demonstrated in Fig. 3b; effects which could lead to an erroneous interpretation of the data. The input GEF data are shown in black. The data are analysed via the 2E-2v method (in red). Some deviations are encountered mainly around mass symmetry. The coincidence requirement (in blue) does not seem to be of major concern. Our simulations shed light on vital aspects of the 2E-2v technique itself and are subject of a dedicated publication under preparation.

3 Double-energy method (2E)

The 2E method is based on the analysis of the measured kinetic energies of both fragments, by momentum conservation. During the iterative analysis, known $\bar{v}(A)$ values must be used [1]. The data on ^{252}Cf are obtained by using a Frisch-grid ionization chamber (FGIC). The chamber is filled with P-10 counting gas, which is ionized when charged fragments are stopped. The total number of electrons is proportional to the deposited energy. Five electrodes are hosted in the chamber; two anodes, two grids and one common cathode where the target is placed. The Frisch-grids provide the emission angle of the fragments relative to the chamber axis. NE-213 equivalent neutron detectors (ND) are used in conjunction with the chamber. Both are put axially to the chamber symmetry axis, effectively reducing the need to determine the azimuthal angle of the fragments relative to the chamber axis. The neutron detectors have an intrinsic threshold for neutrons lying above 0.5 MeV in neutron energy. Both ND are cylindrical in shape and have a size of 102 mm \times 51 mm (diameter \times length). A digital data acquisition was used, storing all signal traces for off-line analysis.

During data analysis the neutron data treatment starts with a calibration both in TOF and pulse-heights (PH). The prompt fission γ peak is utilized for the TOF calibration and for time-walk corrections. The obtained timing resolution is 1.3 ns, determined as the full-width-at-half-maximum of the γ

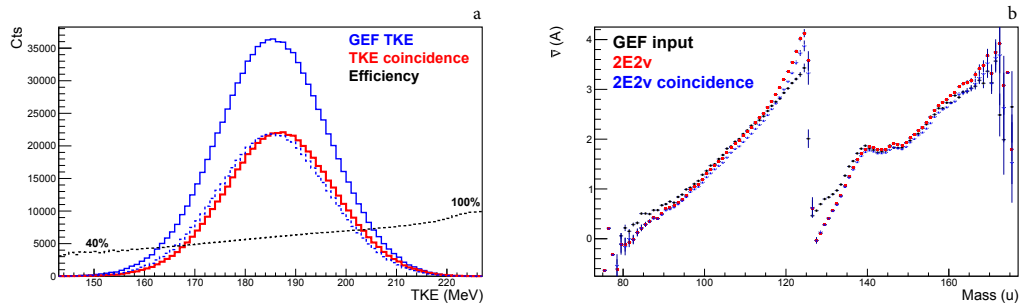


Figure 3. a) TKE distributions from GEF (blue) compared to the TKE for coincident events (red). The dashed line is the TKE from GEF, normalized to the integral of the coincidence data. The black dashed line depicts the ratio between the coincidence data and the input data scaled to 10^4 , revealing a strong energy-dependent efficiency. b) $\bar{\nu}(A)$ from our GEF-simulations. The GEF input data are depicted by the black symbols. The corresponding data obtained from the 2E-2v analysis on the simulated fission events are shown with red symbols, and those requiring coincidences of opposite Si-detector pairs are depicted with the blue symbols.

peak. Secondly, various cuts are applied to the neutron data to discriminate γ rays from neutrons and to correct for neutron scattering. At last, the neutron energy in the laboratory frame is determined and can be used to evaluate the detector intrinsic efficiency relative to the Mannhart ^{252}Cf evaluation (see Ref. [9] and references therein). The FF data are corrected for energy-losses after determining the angular distributions. Iterative calculations lead to the final pre-neutron emission FF mass yields, by using input $\bar{\nu}(A)$ from Ref. [9]. The FF data are corrected for PHD and for the TKE dependence of $\bar{\nu}$ [13]. The fragment-neutron coincidence data, are corrected for the neutron momentum recoil effects. In addition, a cut in the CM system for neutron emission above $\cos(\phi) = 0$ has been applied (where ϕ is the angle between the neutron momentum and the fission axis), in accordance with the approach presented in Ref. [9].

3.1 Results of 2E

Results on ^{252}Cf are shown in Figs. 4a–d. The neutron TOF data are plotted in Fig. 4a, in black after calibration and walk correction. After pulse-shape discrimination using the zero-crossing-method, the blue line shows a much reduced prompt fission γ peak. Further cuts on the TOF removed fully the γ peak as seen in the green curve. Final cuts were applied in the TOF-vs.-PH matrix considering the maximum proton recoil. The clean prompt neutron TOF spectrum is shown in red. The mass distribution is shown in Fig. 4b where the sample side (blue) and backing side (red) are plotted together with the average (green). The distribution is in good agreement with the literature data (in black) but shows a slightly degraded mass resolution. This is due to the ^{252}Cf target, which is of a lower quality (in terms of uniformity of target and backing) compared to the one used in Ref. [9]. In addition, the statistics obtained in this work is significantly lower, which affects the quality of the results. $\bar{\nu}(A)$ is obtained by dividing the coincident mass distribution with the non-coincident one, after normalization for solid angle, total fission rate and proper scaling for $\bar{\nu}_{\text{tot}}$. In Fig. 4c the neutron sawtooth data are drawn, where our data (in red) are in decent agreement to the reference in black. The minimum around 130 u is well reproduced. Small differences can also be seen and could be caused by a lower target quality as well as lower resolution in the neutron TOF measurement. The $\bar{\nu}(\text{TKE})$ is shown in Fig. 4d

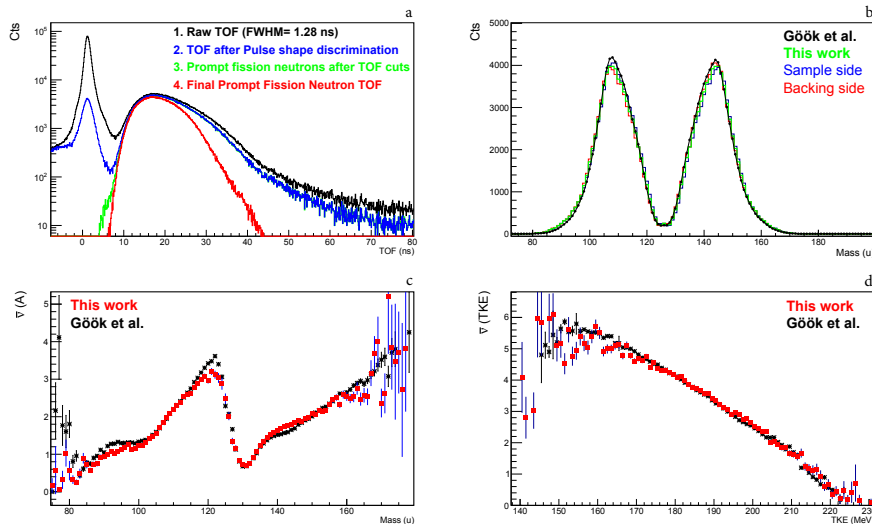


Figure 4. a) The TOF before and after applied cuts (see text for details). b) The 2E mass yields for $^{252}\text{Cf}(\text{sf})$ are shown, for sample and backing sides and their average; c) $\bar{v}(A)$ and d) $\bar{v}(\text{TKE})$. All were compared to Ref. [9].

and exhibits a slope very similar to Ref. [9]. This Cf experiment served as proof-of-principle and the results are quite satisfactory.

These projects were partially financed by EU FP7 CHANDA project, by granting A.A and K.J. scientific visits to the JRC-GEEL. The JRC-GEEL MONNET staff is acknowledged for technical support.

References

- [1] A. Al-Adili et al., Nuclear Data Sheets **119**, 342 (2014)
- [2] D. Doré et al., EPJ Web of Conferences **62**, 05005 (2013)
- [3] J. Matarranz et al, Physics Procedia **47**, 76 (2013)
- [4] K. Meierbachtol et al., Nucl. Instr. and Meth. A **788**, 59 (2015)
- [5] M.O. Frégeau et al., Nucl. Instr. and Meth. A **817**, 35 (2016)
- [6] H.W. Schmitt et al., Phys. Rev. **137**, B837 (1965)
- [7] K. Jansson et al., EPJ Web of Conferences **146**, 04016 (2017)
- [8] R.Müller et al., Phys. Rev. C **29**, 885 (1984)
- [9] A.Göök et al., Phys. Rev. C **90**, 064611 (2014)
- [10] K.Th. Brinkmann et al., Nucl. Instr. and Meth. A **276**, 557 (1989)
- [11] J. Velkovska and R.L. McGrath, Nucl. Instr. and Meth. A **430**, 507 (1999)
- [12] W. Bohne et al., Nucl. Instr. and Meth. A **240**, 145 (1985)
- [13] A. Al-Adili et al., Phys. Rev. C **93**, 034603 (2016)